NASA
TP
1406
c.1

NASA Technical Paper 1406

LOAN COPY: RETURN
AFWL TECHNICAL LIBR
KIRTLAND AFB, N. M
0134802
TECH LIBRARY KAFB, NM

A Modification to Linearized Theory for Prediction of Pressure Loadings on Lifting Surfaces at High Supersonic Mach Numbers and Large Angles of Attack

Harry W. Carlson

FEBRUARY 1979

NASA

TECH LIBRARY KAFB, NM
0134802

NASA Technical Paper 1406

A Modification to Linearized Theory for Prediction of Pressure Loadings on Lifting Surfaces at High Supersonic Mach Numbers and Large Angles of Attack

Harry W. Carlson
Langley Research Center
Hampton, Virginia

National Aeronautics
and Space Administration

**Scientific and Technical
Information Office**

1979

SUMMARY

A study has been made of a new pressure-coefficient formulation based on linearized theory. It is intended to provide more accurate estimates of detailed pressure loadings for improved stability analysis and analysis of critical structural design conditions. The approach is based on the use of oblique-shock and Prandtl-Meyer expansion relationships for accurate representation of the variation of pressures with surface slopes in two-dimensional flow and of linearized-theory perturbation velocities for evaluation of local three-dimensional aerodynamic interference effects. The applicability and limitations of the modification to linearized theory are illustrated through comparisons with experimental pressure distributions for delta wings covering a Mach number range from 1.45 to 4.60 and angles of attack from 0° to 25°. For thin wings at small angles of attack, the modified formulation provides essentially the same pressure-distribution values as the more conventional linearized-theory formulation. However, more accurate overall pressure distributions and wing loadings are provided at moderately high angles of attack and high supersonic Mach numbers.

INTRODUCTION

Linearized-theory methods for the aerodynamic design and analysis of supersonic airplane configurations (refs. 1 to 4, e.g.) have proven to be very useful in the preliminary stages of aircraft design. They provide realistic estimates of aerodynamic performance for reasonably complete airplane configurations. In addition to the wing, these configurations may include a fuselage, tail or canard surfaces, and nacelles or stores. Design details such as wing twist and camber and aerodynamic interference between configuration components are also taken into account. These methods, however, may fail to provide sufficiently accurate estimates of detailed pressure loadings required for stability analysis and for analysis of critical structural design conditions. The problem is most severe for large angles of attack and high supersonic Mach numbers.

The analytic study reported herein provides a modification to linearized theory which is designed to extend the applicability of the local pressure-coefficient prediction to high angles of attack and high supersonic Mach numbers. This is accomplished by means of a new pressure-coefficient formulation for use in existing methods, such as those of references 1 to 4, or in advanced linearized-theory surface-panel methods now being developed, such as those of references 5 and 6. As a first step in a study of the feasibility of the method, the pressure-coefficient formulation has been applied to linearized-theory solutions for delta wings and the results have been compared with experimental pressure distributions.

The approach is based on the observation of two fundamental flaws in linearized theory when applied to delta wings at large angles of attack. The

first is the failure to predict the high local pressures that occur on the wing lower surface in the region of the root chord, where the flow has much of a two-dimensional character. The second is the tendency to predict larger pressure loadings than actually occur in outboard regions of the wing, particularly near the leading edge, where the flow has a highly three-dimensional character. The pressure-coefficient formulation adapted herein attempts to solve these problems by utilization of shock-expansion theory to account for the nonlinear variation of pressure coefficients in two-dimensional flow while retaining the linearized-theory prediction of three-dimensional effects.

SYMBOLS

B,C,D constants used in evaluation of C_p^* (see appendix B)

b wing span

C_N wing normal-force coefficient, $2/S \int_0^{b/2} c_n c \, dy$

C_p pressure coefficient

C_p^* pressure coefficient evaluated by use of the effective deflection angle δ^* (see appendix B)

C_{p,δ_d} pressure coefficient for shock detachment δ_d

$C_{p,\delta=90}$ pressure coefficient for the stagnation pressure behind a normal shock

c local wing chord

c_{av} average wing chord, S/b

c_n section normal-force coefficient, $1/c \int_0^c C_p \, dx'$

$E(k)$ elliptic integral of second kind with modulus k

k modulus of elliptic integral, $\sqrt{1 - \beta_\infty^2 \cot^2 \Lambda}$

l wing overall length (root chord for delta wings)

M^* Mach number corresponding to the effective expansion angle ν^*

M_i local Mach number given by linearized theory in three-dimensional flow (interference included)

M_o	local Mach number given by linearized theory in two-dimensional flow (interference neglected)
M_∞	free-stream Mach number
n	exponent in the expression for M^*
p	static pressure
p_t	total pressure
S	wing area
u,v,w	nondimensional perturbation velocities in Cartesian coordinate system
u_i	nondimensional local longitudinal perturbation velocity given by linearized theory in three-dimensional flow (interference included)
u_o	nondimensional local longitudinal perturbation velocity given by linearized theory in two-dimensional flow (interference neglected)
x,y,z	Cartesian coordinates, origin at wing apex
x'	longitudinal distance behind wing leading edge
x_{cp}	longitudinal center of pressure
y_{cp}	lateral center of pressure
α	angle of attack
β_∞	$= \sqrt{M_\infty^2 - 1}$
γ	ratio of specific heats
δ	flow deflection angle
δ^*	effective flow deflection angle
δ_d	flow deflection angle for shock detachment
ε	lateral flow angle in plane tangent to local surface (see sketch (a))
θ	shock angle for two-dimensional inclined planar surface
θ_d	shock angle for shock detachment
Λ	wing leading-edge sweep angle

λ angle between plane tangent to local surface and free-stream velocity vector (see sketch (a))

λ_i equivalent turning angle due to local perturbation

ν^* Prandtl-Meyer expansion angle for M^*

ν_i Prandtl-Meyer expansion angle for M_i

ν_o Prandtl-Meyer expansion angle for M_o

ν_∞ Prandtl-Meyer expansion angle for M_∞

ϕ angular parameter used in definition of C_p^*

LINEARIZED-THEORY DEFICIENCIES

The failure of linearized theory to provide realistic estimates of pressure distributions at large angles of attack for a high supersonic Mach number is illustrated in figure 1. The experimental data for an uncambered delta wing with the leading edge swept 76° and a 4-percent-thick circular-arc streamwise airfoil section have been taken from reference 5. The theory was evaluated by means of a simple computer program applicable only to delta wings, which is discussed in appendix A. This special computer program, rather than those described in references 1 to 4 or other current methods, was employed to insure a proper evaluation of lateral as well as longitudinal perturbation velocities for linearized-theory calculations. The method of references 1 to 3 does not provide lateral components of velocity v, and the method in reference 4 gives values of v that were found to be in error. More advanced linearized-theory surface-panel methods such as those discussed in references 6 and 7 should provide accurate numerical solutions for all the linearized-theory perturbation velocities.

In figure 1(a), the linearized-theory pressure coefficient has been defined by the standard linearized expression $C_p = -2u$. At the lower angle of attack, which is representative of the normal application of linearized theory, there is a reasonable agreement with the experimental data for all three semispan positions. At the higher angle of attack ($\alpha \approx 20°$), however, there are serious discrepancies. On the wing lower surface, especially in the vicinity of the root chord, the linearized theory fails by a large margin to predict the rather large positive pressures actually attained. In the region of the wing tip upper surface the theory predicts much larger negative pressures than are realized.

A more complete second-order form of the pressure coefficient expression was employed in figure 1(b) to see whether the correlation could be improved by use of all three linearized-theory perturbation velocities. It is evident that the prediction capability has deteriorated. Even the more sophisticated isentropic form of the pressure coefficient employed in figure 1(c) offers an improvement for only the upper surface.

Some fundamental reasons for the failure of linearized theory to predict pressures at large angles of attack may be explored with the aid of figure 2. Here the pressure coefficient on a planar surface inclined to the free-stream flow is shown as a function of the flow deflection angle δ for six supersonic Mach numbers. For this situation the linearized-theory pressure coefficient without interference is given as $C_p = 2\delta/\beta$ (where δ is in radians). The more exact oblique-shock compression and Prandtl-Meyer expansion relationships (which are hereinafter referred to as shock-expansion relationships) from reference 8, however, show a far from linear variation with the deflection angle. For positive deflections, the pressure coefficient increases at an ever greater rate with increasing deflection until the shock detachment angle δ_d is reached. At this point the flow becomes locally subsonic and the purely supersonic prediction methods are no longer applicable. Note the small angles at which shock detachment occurs for the low supersonic Mach numbers. This makes the problem of pressure prediction at high angles of attack and low supersonic Mach numbers extremely difficult. For negative deflection angles, the pressure coefficients given by the expansion relationships show a far slower growth of negative pressure than do those given by the linearized theory. In fact, a limiting or vacuum pressure coefficient defined as $-2/\gamma M_\infty^2$ is approached. The shock-expansion and linearized-theory curves are coincident only at $\delta = 0^\circ$. Figure 2 thus depicts clearly the major reasons for the linearized-theory failures: both the underprediction of positive pressures on the lower surface and the overprediction of negative pressures on the upper surface of a wing at high angles of attack.

THEORY MODIFICATION

The preceding analysis led to consideration of a theoretical pressure-coefficient formulation which combines the more exact, two-dimensional, interference-free prediction capabilities of the shock-expansion relationships with the linearized-theory capabilities for handling of three-dimensional interference effects. In brief, a local pressure coefficient C_p^*, is calculated in accordance with the shock-expansion relationships for an effective deflection angle δ^*. This effective deflection angle includes a purely geometric component (based on the local-surface slope relative to the free stream) and an aerodynamic interference component (based on local interference velocities evaluated by normal linearized-theory methods). Thus,

$$\delta^* = \lambda + \lambda_i \tag{1}$$

where λ is the angle between a plane tangent to the local surface and the free-stream velocity vector and λ_i is an equivalent turning angle due to differences between local perturbation velocities and interference-free values.

The equivalent turning angle is defined from Prandtl-Meyer expansion equations as

$$\lambda_i = \nu_o - \nu_i \tag{2}$$

where

$$\nu_o = \sqrt{6}\,\tan^{-1}\sqrt{\frac{M_o^2 - 1}{6}} - \cos^{-1}\left(\frac{1}{M_o}\right)$$

$$\nu_i = \sqrt{6}\,\tan^{-1}\sqrt{\frac{M_i^2 - 1}{6}} - \cos^{-1}\left(\frac{1}{M_i}\right)$$

and

$$M_o = M_\infty(1 + u_o)$$

$$M_i = M_\infty \frac{(1 + u_i)}{\cos \varepsilon}$$

In the above expressions u_o is the longitudinal perturbation velocity without interference, u_i is the longitudinal perturbation velocity including interference, and ε is the lateral flow angularity on a local surface inclined at an angle λ with respect to the free stream. The angles λ and ε are depicted in sketch (a):

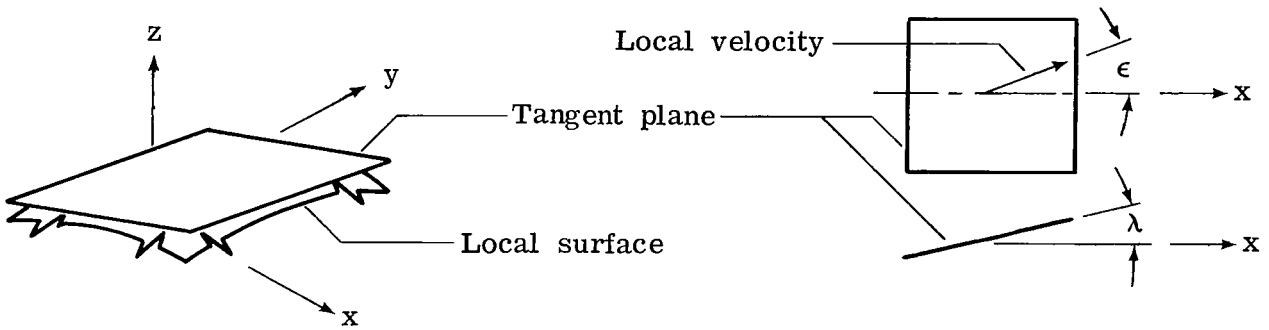

Sketch (a)

Because linearized theory allows the longitudinal perturbation velocities to approach negative infinity instead of the more realistic limit of -1 (which corresponds to a stagnation point), an arbitrary constraint defined by the following equations has been introduced:

$$u_o = -\frac{\lambda}{\beta_\infty} \qquad (\lambda < 0) \qquad (3)$$

$$u_o = 1 - \frac{2}{\left(\frac{1}{1 + \frac{\lambda}{\beta_\infty}\frac{\pi}{180}}\right)^2 + 1} \qquad (\lambda > 0) \qquad (4)$$

$$u_i = u \qquad (u > 0) \qquad (5)$$

$$u_i = 1 - \frac{2}{\left(\frac{1}{1 - u}\right)^2 + 1} \qquad (u < 0) \qquad (6)$$

This adjustment limits M_o and M_i to values greater than zero.

Values of δ^* calculated according to the procedure just outlined are used to define a local pressure coefficient C_p^* through use of the shock-expansion relationships in reference 8. These equations as adopted for the present purposes are given in appendix B. A typical variation of C_p^* with δ^* is shown in sketch (b):

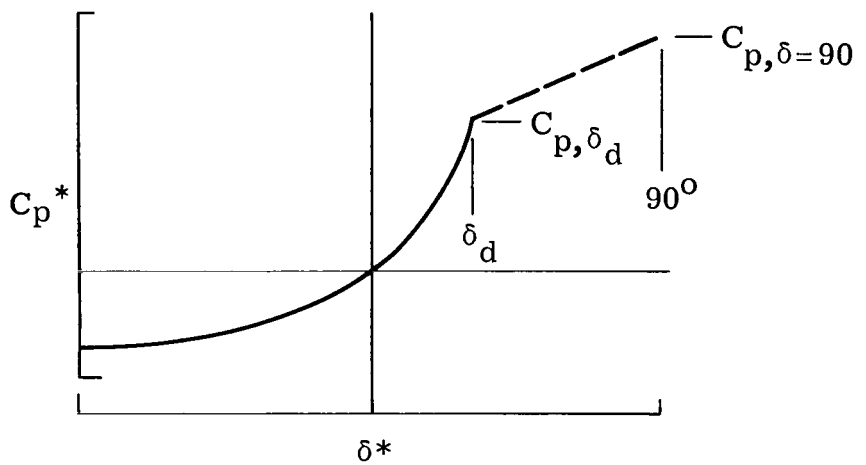

Sketch (b)

When the local Mach numbers M_o or M_i become less than 1, the Prandtl-Meyer expansion equations are no longer applicable, and without special provisions the whole calculation process would have to be terminated. Therefore, provision has been made to provide fictitious expansion angles for local Mach numbers less than 1 so that the process may continue. For M_o and M_i less than 1, the expansion angles are defined as

$$\nu_o = (\nu_\infty - 90)(1 - M_o)^2 \tag{7}$$

$$\nu_i = (\nu_\infty - 90)(1 - M_i)^2 \tag{8}$$

Normally, this provision is not employed unless the local surface slope exceeds by an appreciable margin the shock detachment angle δ_d for the free-stream Mach number. In programming this procedure for the examples in this report, care was taken to indicate each incidence of M_o and M_i less than 1 so that the impact on the overall solution could be assessed.

RESULTS AND DISCUSSION

The linearized-theory modification discussed in the previous section has been applied to delta wings for which experimental pressure distributions are available. For the present, application of the method is restricted to uncambered wings of delta or arrow planform, because existing linearized-theory methods applicable to wings of arbitrary planform and arbitrary surface shape do not appear to provide correct values of all the perturbation velocities. Advanced linearized-theory methods utilizing surface panels with continuous distributions of singularities (refs. 6 and 7) should remedy this situation.

For the delta wings treated here, the linearized-theory perturbation velocities were determined from a computer program created especially for this purpose. The program is based on the equations given in reference 9 and listed in appendix A. Velocities determined from these equations were then employed in the definition of a modified linearized-theory pressure coefficient as described in the section "Theory Modification" and in appendix B. The flow angularity ε in the local surface tangent plane was assumed to be simply $\tan^{-1} v$.

Chordwise pressure distributions from reference 5 for a delta wing with the leading edge swept 76° and 4-percent-thick circular-arc streamwise airfoil sections are presented in figure 3. Data were taken at Mach numbers of 2.3, 3.5, and 4.6 and at angles of attack up to about 20°. The Mach numbers and angles of attack shown here are representative of those for which the modification to linearized theory would be expected to apply. The effective deflection angle δ^* is in all cases less than the maximum deflection angle for shock detachment δ_d. At deflections greater than δ_d, the flow is not supersonic everywhere and the modification becomes invalid.

In all parts of figure 3, the wing lower-surface pressures along the root chord $y/(b/2) = 0$ are better predicted by the modified formulation for the pressure coefficient. At the root chord, where the v-components of perturbation velocity are zero, the improved pressure-coefficient prediction is due to the nonlinear nature of the shock-expansion relationships. As a matter of interest, it might be noted that the interference component λ_i of the effective deflection angle δ^* plays an important role. Without this term the midchord lower-surface pressure coefficient at the highest angle of attack would be 0.545 at $M_\infty = 2.3$ and 0.372 at $M_\infty = 4.6$. At the outboard station $y/(b/2) = 0.8$ the upper-surface pressures are better predicted by the modifi-

cation to linearized theory because the shock-expansion relationships account for the vacuum pressure limitation $-2/\gamma M_\infty^2$.

For the lower surface of the outboard station, the modified formulation provides an improvement in the overall shape of the distribution, but provides only a marginal improvement in the general level. Perhaps most significant here is that the modified formulation eliminates the infinite pressures of the wing leading edges for subsonic leading edges ($M_\infty = 2.3$ and $M_\infty = 3.5$). Because of the strong sidewash, or v contribution, the lower-surface leading-edge pressures defined by the modified C_p formulation approach the vacuum limit. At moderate angles of attack, the experimental data show evidence of the formation of a separated leading-edge vortex flow pattern on the wing upper surface. Note especially the data for $\alpha = 9.94^\circ$ and $y/(b/2) = 0.4$ at a Mach number of 2.3. It is possible that the modified pressure-coefficient formulation in combination with vortex flow prediction methods, such as that of reference 10, could provide good predictions of local pressures for this phenomenon. Large sidewash velocities on the wing surface caused by the separated vortex could well cause an approach to the limiting vacuum pressure coefficient, which is -0.270 for this Mach number of 2.3.

Spanwise loading distributions for the 76° delta wings at all three Mach numbers are shown in figure 4. The loadings predicted by the modified C_p formulation provide a better description of the experimental loading distribution at the higher angles of attack and at the higher Mach numbers. At the lower angles, the newer method offers little or no benefit.

Force data for the same 76° delta wings from reference 5 are shown in figure 5. For the wing normal-force coefficient, there is little difference between the two approaches. A well-known characteristic of the simple linearized theory is its ability to predict overall forces in spite of sometimes large failures in prediction of detailed pressure distributions. The modified system does, however, offer an improvement in prediction of longitudinal center of pressure.

Data for a delta wing with the leading edge swept 63.4° at angles of attack of 6°, 15°, and 25° (refs. 11 and 12) are presented in figure 6. The wing streamwise sections were modified biconvex with maximum thickness ratios of 5 percent at midchord and with 50-percent-blunt trailing edges. For the Mach numbers of 2.46 and 3.36, results differ little from those for the 76° swept wing and no new conclusions may be drawn. The supersonic-leading-edge condition at lower Mach numbers creates no particular problem. At a Mach number of 1.97, the results at $\alpha = 6^\circ$ and $\alpha = 15^\circ$ are similar to those shown previously. However at $\alpha = 25^\circ$, there are some regions of the wing (e.g., the lower surface near the apex) where the effective deflection angle δ^* becomes larger than the shock separation angle δ_d, an indication that the real problem is one of a mixed subsonic and supersonic flow. For this angle there is some deterioration in the correlation between the modified formulation values and the experimental data.

At the lowest Mach number of 1.45 and at an angle of attack of 15°, δ^* is larger than the δ_d value of 10.8° for most of the forward half of the wing chord for all the stations shown. This is indicated by the break in the modi-

fied formulation curve. All data ahead of this point result from an arbitrary description of C_p^* versus δ^*, as discussed in appendix B. Of course, the presence of such a large region of indicated subsonic flow invalidates any supersonic linearized-theory solution. This is really a mixed, or transonic, flow problem. The good agreement between the predicted values and the measured data at $\alpha = 25^\circ$ is entirely fortuitous, because δ^* is larger than δ_d for all the data shown. Only for $\alpha = 6^\circ$ is the linearized theory valid. Here, there is little difference between the two C_p formulations.

Spanwise distributions of normal force for the 63.4° swept wing are shown in figure 7. For the higher Mach numbers, the predictions given by the modified formulation appear to be reasonable and offer an improvement over the simpler linearized formulation. Integrated force data for this wing are shown in figure 8. As indicated previously, the newer approach is not expected to offer any improvement at the lower Mach number. At the higher Mach numbers there is little difference in normal force for the two formulations, but the modified formulation does offer an improvement in center of pressure location.

In a further attempt at defining the limits of applicability of the modified method, correlations with pressure distribution data from reference 13 at Mach numbers of 1.61 and 2.01 for a delta wing with the leading edge swept 70° are shown in figure 9. This wing had NACA 65A003 streamwise airfoil sections. The rounded leading edge thus assured that for all angles of attack there would be some portion of the wing subject to subsonic flow. Only in the vicinity of the wing apex for a Mach number of 1.61 and an angle of attack of 20° is there evidence of an appreciable discrepancy between experimental data and values predicted by the modified formulation resulting from local subsonic flow. For this Mach number the shock detachment angle is 14.9°. At a Mach number of 2.01, where the highest angle of attack (20°) is less than the shock detachment angle of 23.1°, good correlation between predictions by the modified formulation and the experimental data is shown for all the data presented. Apparently the rounded leading edge introduces only localized regions of subsonic flow and does not invalidate the present modification to linearized theory.

In general, the correlations presented here indicate an applicability range of the present modification to linearized theory limited by angles of attack roughly equal to the shock detachment angle for a given Mach number. Outside this range of applicability the problem of pressure distribution prediction actually involves mixed supersonic and subsonic (transonic) flow phenomena and thus is not amenable to any theories which assume all supersonic flow.

After writing this paper, the author became aware of another method being advanced for the combining of linearized-theory and shock-expansion formulations. This other work, reported in reference 14 is based on the same general premise, but differs considerably in implementation. It is intended primarily for hypersonic Mach numbers in the range $M_\infty = 4$ to 8.

CONCLUSIONS

A study has been made of a new linearized-theory formulation for the prediction of pressure coefficients on lifting surfaces at high supersonic Mach numbers and large angles of attack. The formulation is based on the use of shock-expansion relationships for accurate representation of the variation of pressures with surface slopes in two-dimensional flow and the use of linearized-theory perturbation velocities for evaluation of local three-dimensional aerodynamic interference effects. The study has led to the following conclusions:

1. The new pressure-coefficient formulation generally provides a more accurate representation of local pressure coefficients and section normal-force distributions for moderately high angles of attack and high supersonic Mach numbers than does the conventional linearized-theory formulation, although the changes in overall wing normal forces are negligible.

2. At small angles of attack, for the relatively thin wings treated, differences between the modified formulation and the more conventional linearized-theory formulation are small.

3. In general, the applicability range of the modification to linearized theory is limited to angles of attack roughly equal to the shock detachment angle for a given Mach number. Outside this range of applicability, the problem of pressure distribution prediction involves mixed supersonic and subsonic (transonic) flow, and thus is not amenable to any theories which assume all supersonic flow.

Langley Research Center
National Aeronautics and Space Administration
Hampton, VA 23665
January 25, 1979

APPENDIX A

LINEARIZED THEORY FOR DELTA WINGS

The u- and v-components of perturbation velocity for calculation of pressure coefficients by linearized theory were found by means of a computer program based on equations presented in reference 9. The thickness solution for arbitrary wing sections was assembled by well-known superposition techniques. Longitudinal components of perturbation velocity u were found by direct application of equations presented in reference 9. Special techniques were required to find lateral perturbation velocity components v. The expressions for u are listed first.

Perturbation velocities due to thickness -

Supersonic leading edges:

$$u = \frac{-\lambda \cot \Lambda}{\sqrt{\beta_\infty^2 \cot^2 \Lambda - 1}} \qquad (x < \beta_\infty y) \qquad (9)$$

$$u = \frac{-\lambda \cot \Lambda}{\sqrt{\beta_\infty^2 \cot^2 \Lambda - 1}} \left[1 - \frac{2}{\pi} \sin^{-1} \sqrt{\frac{1 - (\beta_\infty^2 y^2/x^2)}{\beta_\infty^2 \cot^2 \Lambda - (\beta_\infty^2 y^2/x^2)}} \right] \qquad (x > \beta_\infty y) \qquad (10)$$

Subsonic leading edges:

$$u = \frac{-2\lambda \cot \Lambda}{\pi \sqrt{1 - \beta_\infty^2 \cot^2 \Lambda}} \cosh^{-1} \sqrt{\frac{1 - \beta_\infty^2 \cot^2 \Lambda}{(\beta_\infty^2 y^2/x^2) - (\beta_\infty^2 \cot^2 \Lambda)}} \qquad (x < y \tan \Lambda) \qquad (11)$$

$$u = \frac{-2\lambda \cot \Lambda}{\pi \sqrt{1 - \beta_\infty^2 \cot^2 \Lambda}} \cosh^{-1} \sqrt{\frac{1 - (\beta_\infty^2 y^2/x^2)}{(\beta_\infty^2 \cot^2 \Lambda) - (\beta_\infty^2 y^2/x^2)}} \qquad (x > y \tan \Lambda) \qquad (12)$$

Perturbation velocities due to lift -

Supersonic leading edges:

$$u = \frac{\alpha \cot \Lambda}{\sqrt{\beta_\infty^2 \cot^2 \Lambda - 1}} \qquad (x < \beta_\infty y) \qquad (13)$$

APPENDIX A

$$u = \frac{\alpha \cot \Lambda}{\sqrt{\beta_\infty{}^2 \cot^2 \Lambda - 1}}\left[1 - \frac{2}{\pi} \sin^{-1}\sqrt{\frac{1 - (\beta_\infty{}^2 y^2/x^2)}{\beta_\infty{}^2 \cot^2 \Lambda - (\beta_\infty{}^2 y^2/x^2)}}\right] \qquad (x > \beta_\infty y) \qquad (14)$$

Subsonic leading edges:

$$u = \frac{\alpha \cot \Lambda}{E(k)} \frac{\beta_\infty \cot \Lambda}{\sqrt{\beta_\infty{}^2 \cot^2 \Lambda - (\beta_\infty{}^2 y^2/x^2)}} \qquad (x > \beta_\infty y) \qquad (15)$$

where

$$k = \sqrt{1 - \beta_\infty{}^2 \cot^2 \Lambda}$$

No direct solutions for v were found in the literature. However, for the lifting velocities with subsonic leading edges, it was possible to derive an analytic expression for v by an integration to obtain the velocity potential and a subsequent differentiation to obtain v. For that case

$$v = \frac{\alpha}{E(k)} \frac{\beta_\infty y/x}{\sqrt{\beta_\infty{}^2 \cot^2 \Lambda - (\beta_\infty{}^2 y^2/x^2)}} \qquad (x > \beta_\infty y) \qquad (16)$$

Because analytic expressions could not be found for the other conditions, v was found by numerical means for all conditions, and v for that one special case was used only as a check on the numerical accuracy. It was found through geometric considerations for wings with conical flow that v could be expressed as a function of an integral of u in a simple equation:

$$v = \frac{1}{y}\int_0^{x'} u\, dx' - \frac{x}{y} u(x') \qquad (17)$$

This expression in combination with the previously defined equations for u were programmed on a high-speed digital computer to obtain linearized-theory solutions for the correlation examples presented in this report.

APPENDIX B

PRESSURE COEFFICIENT DEFINITION BY SHOCK-EXPANSION RELATIONSHIPS

Nearly exact expressions for the pressures acting on the surfaces of planes inclined with respect to the free-stream flow have been defined in reference 8. These expressions are used in this appendix to calculate a modified pressure coefficient C_p^* as a function of the effective deflection angle δ^* given in the section "Theory Modification."

First, it is necessary to define the shock detachment angle for the free-stream Mach number. The shock angle for detachment θ_d is

$$\theta_d = \sin^{-1}\sqrt{\frac{1}{7M_\infty^2}\left[3M_\infty^2 - 2 + \sqrt{3(3M_\infty^4 - 4M_\infty^2 + 13)}\right]} \tag{18}$$

From this, the surface slope for shock detachment δ_d can be calculated:

$$\delta_d = \tan^{-1}\left[\frac{5(M_\infty^2 \sin 2\theta_d - 2\cot\theta_d)}{10 + M_\infty^2(7 + 5\cos 2\theta_d)}\right] \tag{19}$$

For δ^* values greater than 0 but less than δ_d, C_p^* can be calculated by a process suggested in reference 8 and implemented in reference 15. The process requires a three-step operation:

$$\phi = \cos^{-1}\left[\frac{4.5BC - B^3 - 13.5D}{(B^2 - 3C)^{3/2}}\right] \tag{20}$$

$$\theta = \sin^{-1}\sqrt{\frac{-B}{3} + \frac{2}{3}\sqrt{B^2 - 3C}\cos\left(\frac{\phi + 4\pi}{3}\right)} \tag{21}$$

$$C_p^* = \frac{5}{3}\left(\frac{M_\infty^2 \sin^2\theta - 1}{M_\infty^2}\right) \tag{22}$$

where

$$B = -\left(\frac{M_\infty^2 + 2}{M_\infty^2}\right) - 1.4 \sin^2 \delta^*$$

$$C = \frac{2M_\infty^2 + 1}{M_\infty^4} + \left(1.44 + \frac{0.4}{M_\infty^2}\right) \sin^2 \delta^*$$

$$D = -\frac{\cos^2 \delta^*}{M_\infty^4}$$

For δ^* values greater than δ_d, no valid solution can be found because the local Mach number becomes subsonic. The problem then involves a mixed supersonic and subsonic flow and neither supersonic linearized-theory nor shock-expansion relationships are applicable. Because only a small portion of the flow may be affected in many cases, calculations for the examples shown in this report were not terminated when δ^* became larger than δ_d. Instead, an arbitrary linear fairing between the pressure coefficient for shock detachment C_{p,δ_d} and the pressure coefficient corresponding to the stagnation pressure behind a normal shock $C_{p,\delta=90}$ was introduced. Thus, for δ^* greater than δ_d,

$$C_p^* = C_{p,\delta_d} + \left(C_{p,\delta=90} - C_{p,\delta_d}\right) \frac{\delta^* - \delta_d}{90 - \delta_d} \tag{23}$$

where

$$C_{p,\delta_d} = \frac{5}{3}\left(\frac{M_\infty^2 \sin^2 \theta_d - 1}{M_\infty^2}\right)$$

and

$$C_{p,\delta=90} = \left[\left(1.2M_\infty^2\right)^{3.5}\left(\frac{6}{7M_\infty^2 - 1}\right)^{2.5} - 1\right]\frac{1}{0.7M_\infty^2}$$

In the programming, provision was made to indicate each incidence of δ^* in excess of δ_d so that the impact on the overall solution could be assessed.

APPENDIX B

For δ^* values less than 0, Prandtl-Meyer expansion relationships were employed. First, an effective expansion angle ν^* is defined:

$$\nu^* = \nu_\infty - \delta^* \tag{24}$$

where

$$\nu_\infty = \sqrt{6}\ \tan^{-1}\sqrt{\frac{M_\infty^2 - 1}{6}} - \cos^{-1}\frac{1}{M_\infty}$$

Then an effective expansion Mach number may be defined. No direct expression for Mach number as a function of expansion angle was found in the literature. However, an effective expansion Mach number may be approximated by

$$M^* = \frac{1}{1 - \left(\frac{\nu^*}{130.45}\right)^n} \tag{25}$$

where

$$n = 0.56 + 0.313\left(\frac{\nu^*}{130.45}\right) - 0.42\sqrt{\frac{\nu^*}{130.45}}$$

and ν^* is in degrees. This approximation has Mach number errors of no more than 0.005 in the Mach number range of 1.0 to 10.0. With ν^* and M^* defined, $C_p{}^*$ may be found from

$$C_p{}^* = \frac{1}{0.7M_\infty^2}\left[\frac{p/p_t(M^*,\nu^*)}{p/p_t(M_\infty,\nu_\infty)} - 1\right] \tag{26}$$

where

$$\frac{p}{p_t}(M^*,\nu^*) = \left(\frac{1}{2.4}\left\{1 + \cos\left[\frac{2}{\sqrt{6}}\left(\nu^* + \cos^{-1}\frac{1}{M^*}\right)\right]\right\}\right)^{3.5}$$

APPENDIX B

$$\frac{p}{p_t}(M_\infty, \nu_\infty) = \left(\frac{1}{2.4} \left\{ 1 + \cos \left[\frac{2}{\sqrt{6}} \left(\nu_\infty + \cos^{-1} \frac{1}{M_\infty} \right) \right] \right\} \right)^{3.5}$$

REFERENCES

1. Middleton, W. D.; and Lundry, J. L.: A Computational System for Aerodynamic Design and Analysis of Supersonic Aircraft. Part 1 - General Description and Theoretical Development. NASA CR-2715, 1976.

2. Middleton, W. D.; Lundry, J. L.; and Coleman, R. G.: A Computational System for Aerodynamic Design and Analysis of Supersonic Aircraft. Part 2 - User's Manual. NASA CR-2716, 1976.

3. Middleton, W. D.; Lundry, J. L.; and Coleman, R. G.: A Computational System for Aerodynamic Design and Analysis of Supersonic Aircraft. Part 3 - Computer Program Description. NASA CR-2717, 1976.

4. Woodward, F. A.: An Improved Method for the Aerodynamic Analysis of Wing-Body-Tail Configurations in Subsonic and Supersonic Flow. NASA CR-2228, Pts. I-II, 1973.
   Part I - Theory and Application.
   Part II - Computer Program Description.

5. Sorrels, Russell B., III; and Landrum, Emma Jean: Theoretical and Experimental Study of Twisted and Cambered Delta Wings Designed for a Mach Number of 3.5. NASA TN D-8247, 1976.

6. Erickson, Larry L.; Johnson, Forrester T.; and Ehlers, F. Edward: Advanced Surface Paneling Method for Subsonic and Supersonic Flow. Proceedings of the SCAR Conference - Part 1, NASA CP-001, [1977], pp. 25-54.

7. Woodward, Frank A.; and Landrum, Emma Jean: The Supersonic Triplet - A New Aerodynamic Panel Singularity With Directional Properties. AIAA Paper No. 790273, Jan. 1979.

8. Ames Research Staff: Equations, Tables, and Charts for Compressible Flow. NACA Rep. 1135, 1953.

9. Puckett, A. E.; and Stewart, H. J.: Aerodynamic Performances of Delta Wings at Supersonic Speeds. J. Aeronaut. Sci., vol. 14, no. 10, Oct. 1947, pp. 567-578.

10. Gloss, Blair B.; and Johnson, Forrester T.: Development of an Aerodynamic Theory Capable of Predicting Surface Loads on Slender Wings With Vortex Flow. Proceedings of the SCAR Conference - Part 1, NASA CP-001, [1977], pp. 55-67.

11. Kaattari, George E.: Pressure Distributions on Triangular and Rectangular Wings to High Angles of Attack - Mach Numbers 1.45 and 1.97. NACA RM A54D19, 1954.

12. Kaattari, George E.: Pressure Distributions on Triangular and Rectangular Wings to High Angles of Attack - Mach Numbers 2.46 and 3.36. NACA RM A54J12, 1955.

13. Landrum, Emma Jean: A Tabulation of Wind-Tunnel Pressure Data and Section Aerodynamic Characteristics at Mach Numbers of 1.61 and 2.01 for Two Trapezoidal and Three Delta Wings Having Different Surface Shapes. NASA TN D-1394, 1962.

14. Brooke, D.; and Vondrasek, D. V.: Feasibility of Combining Linear Theory and Impact Theory Methods for the Analysis and Design of High Speed Configurations. NASA CR-3069, 1979.

15. Mascitti, Vincent R.: A Closed-Form Solution to Oblique Shock-Wave Properties. J. Aircr., vol. 6, no. 1, Jan.-Feb. 1969, p. 66.

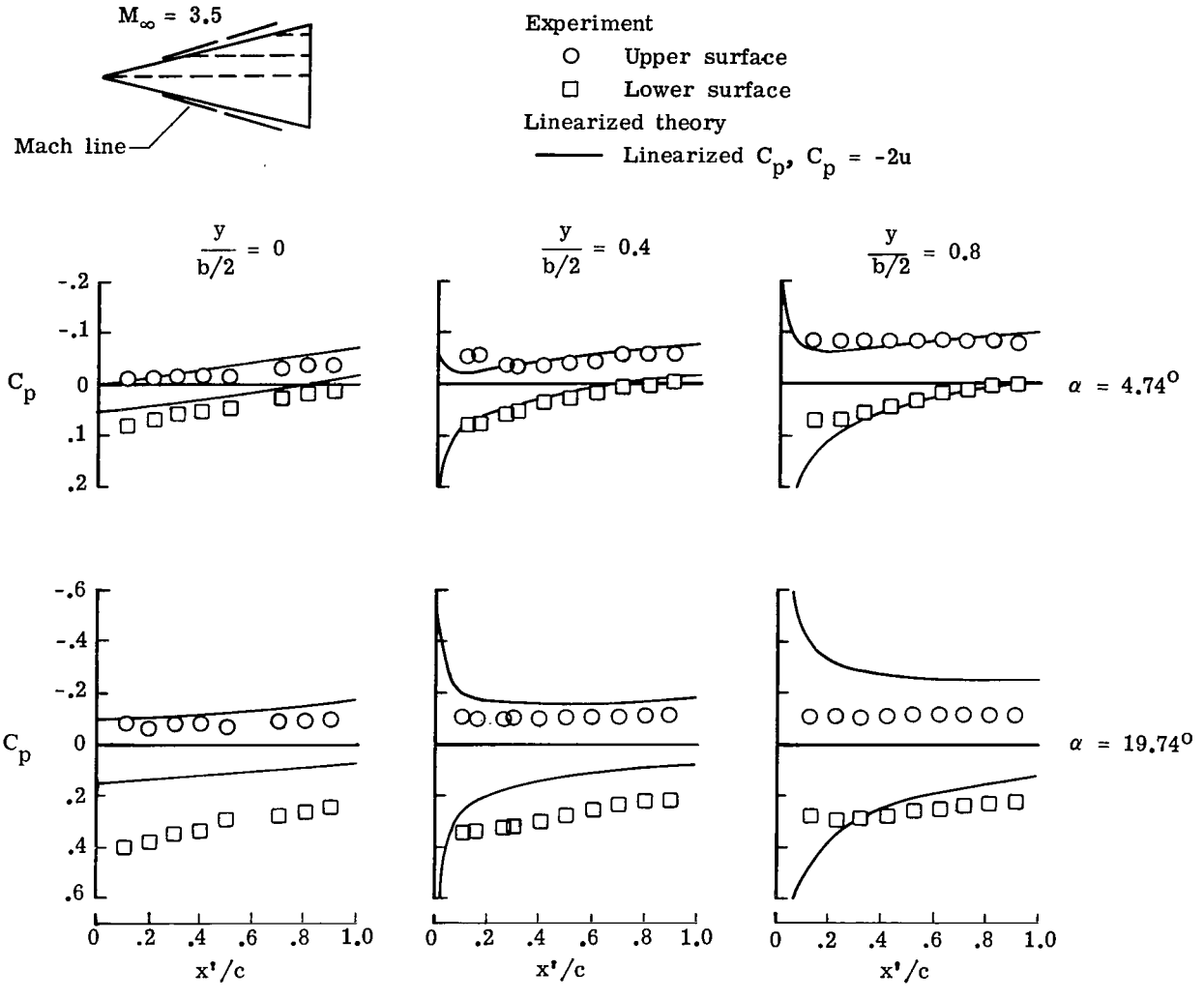

(a) Linearized C_p.

Figure 1.- An illustration of failure of linearized theory to predict pressure distributions for large angles of attack. Delta wing with leading edge swept 76°; M_∞ = 3.5 (ref. 5).

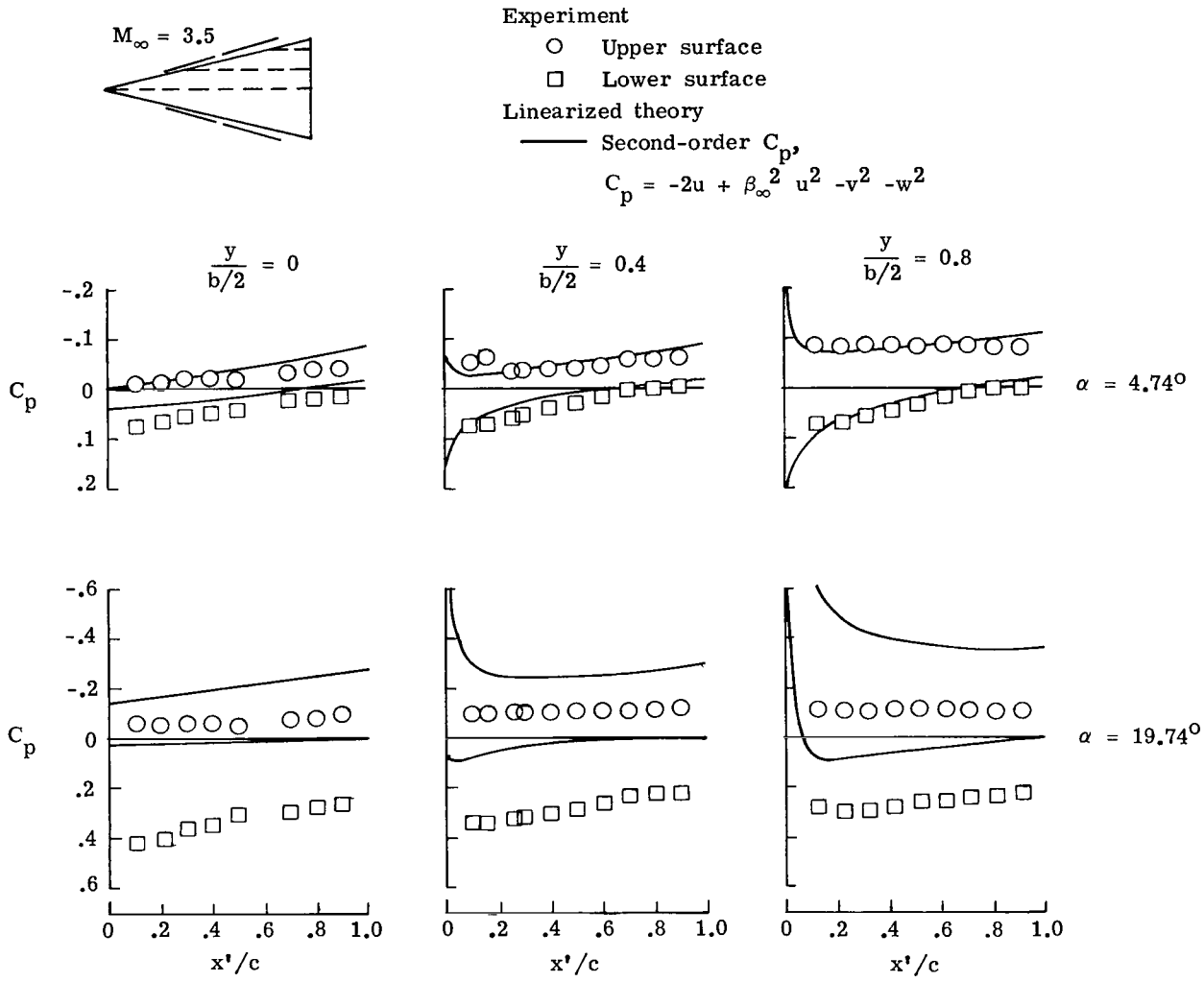

(b) Second-order C_p.

Figure 1.- Continued.

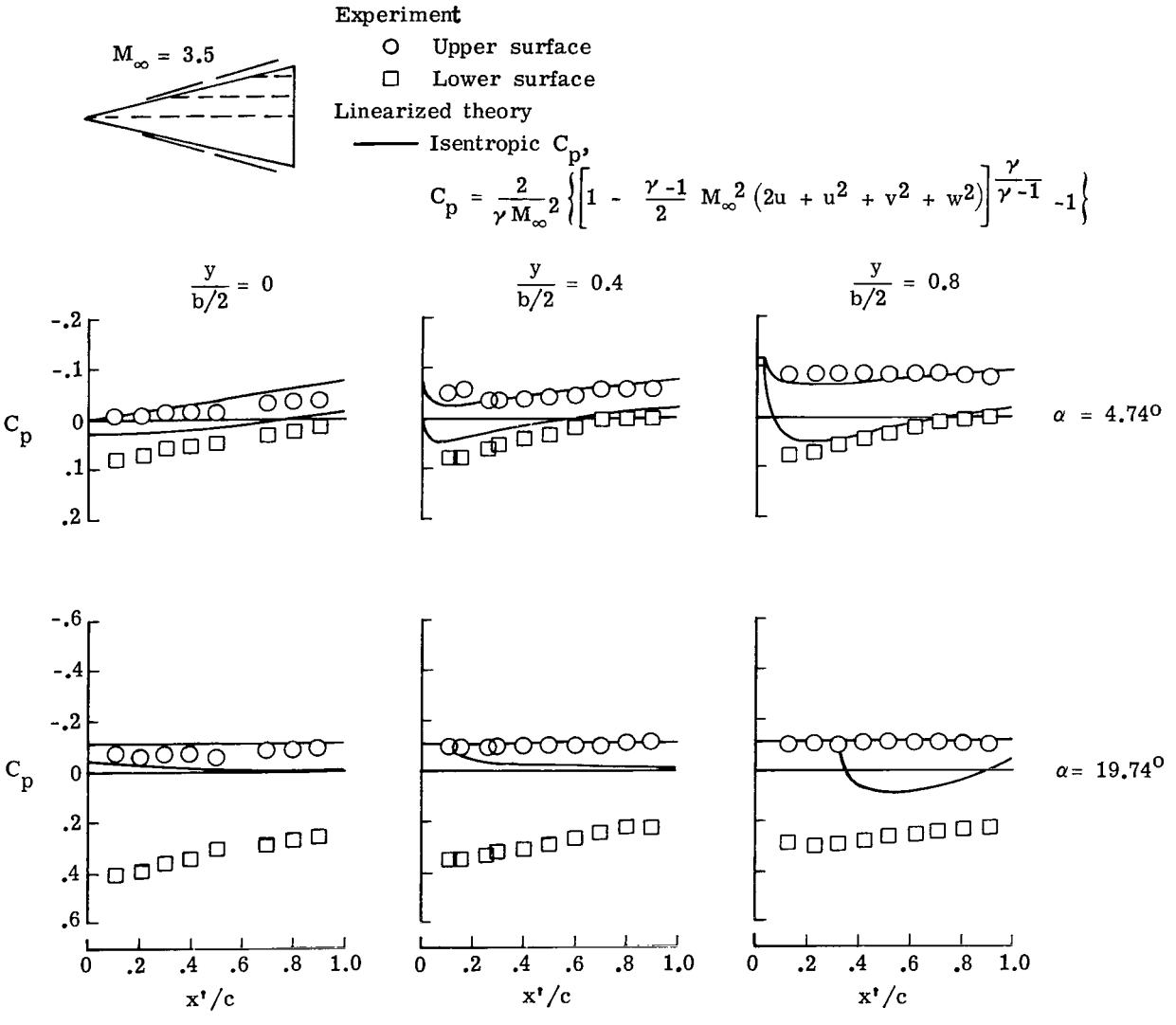

(c) Isentropic C_p.

Figure 1.- Concluded.

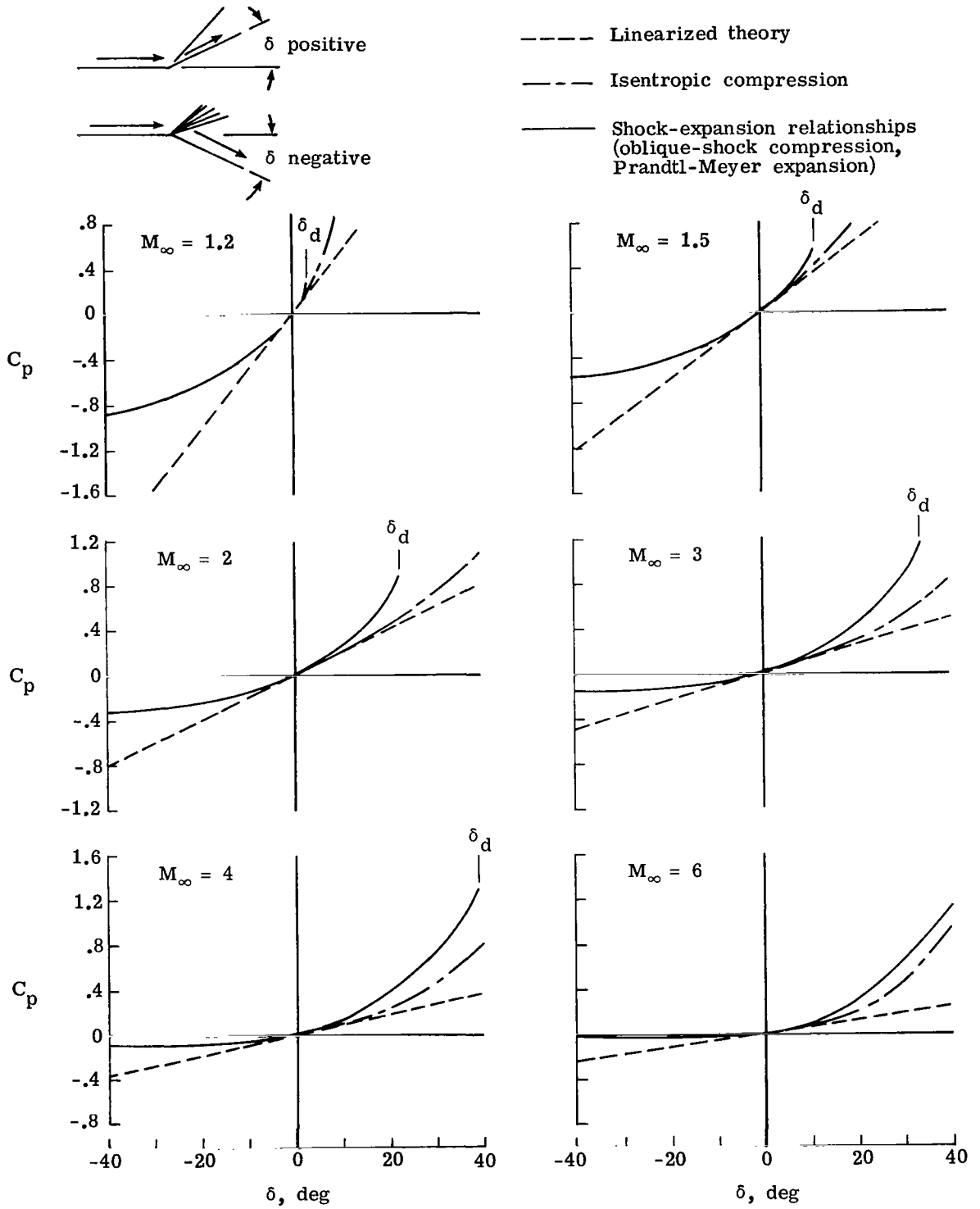

Figure 2.- Pressure coefficient as a function of flow deflection angle for two-dimensional flow.

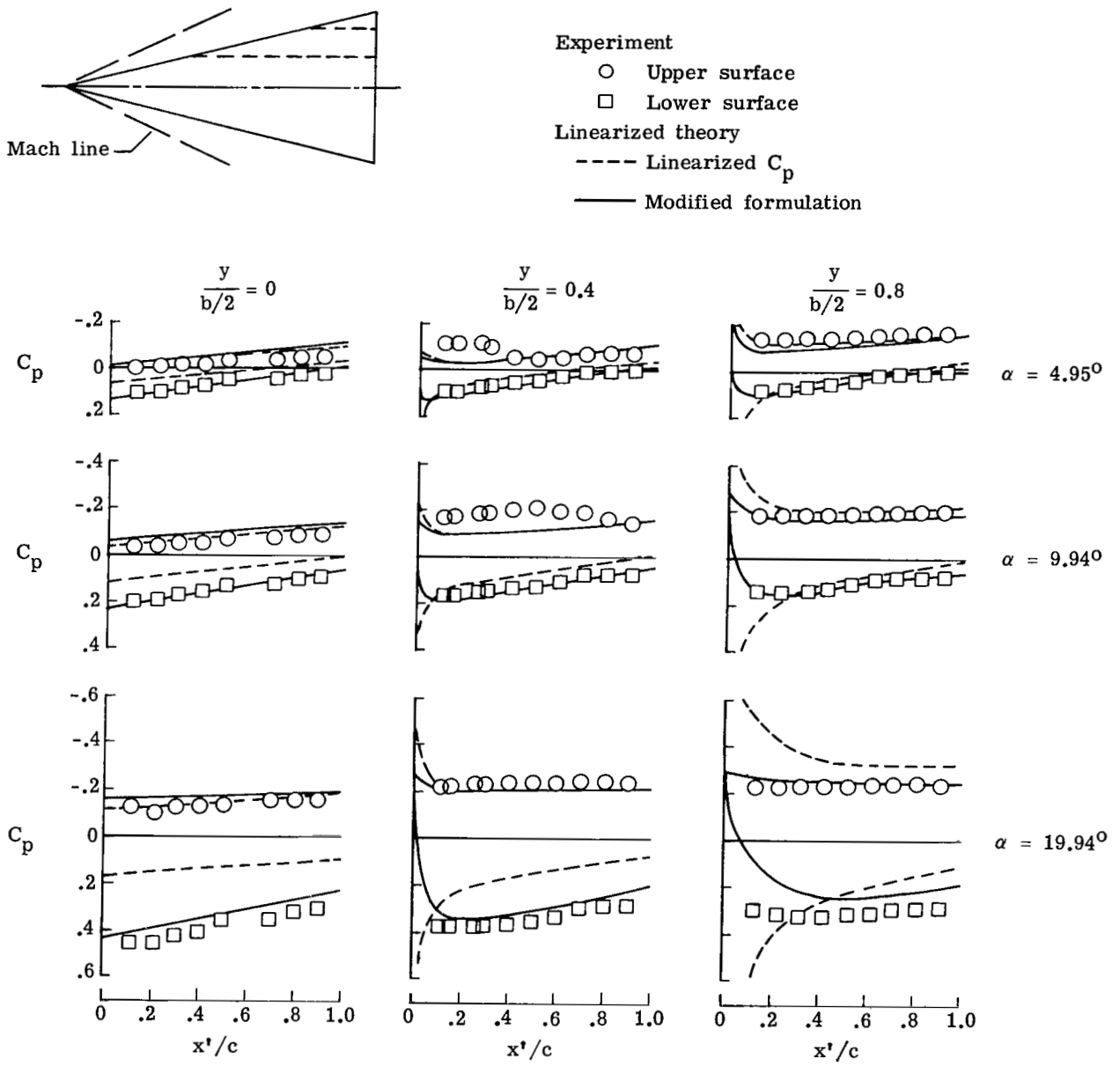

(a) $M_\infty = 2.3$.

Figure 3.- Comparison of predicted and measured pressure distributions for a delta wing with leading edge swept 76° (ref. 5).

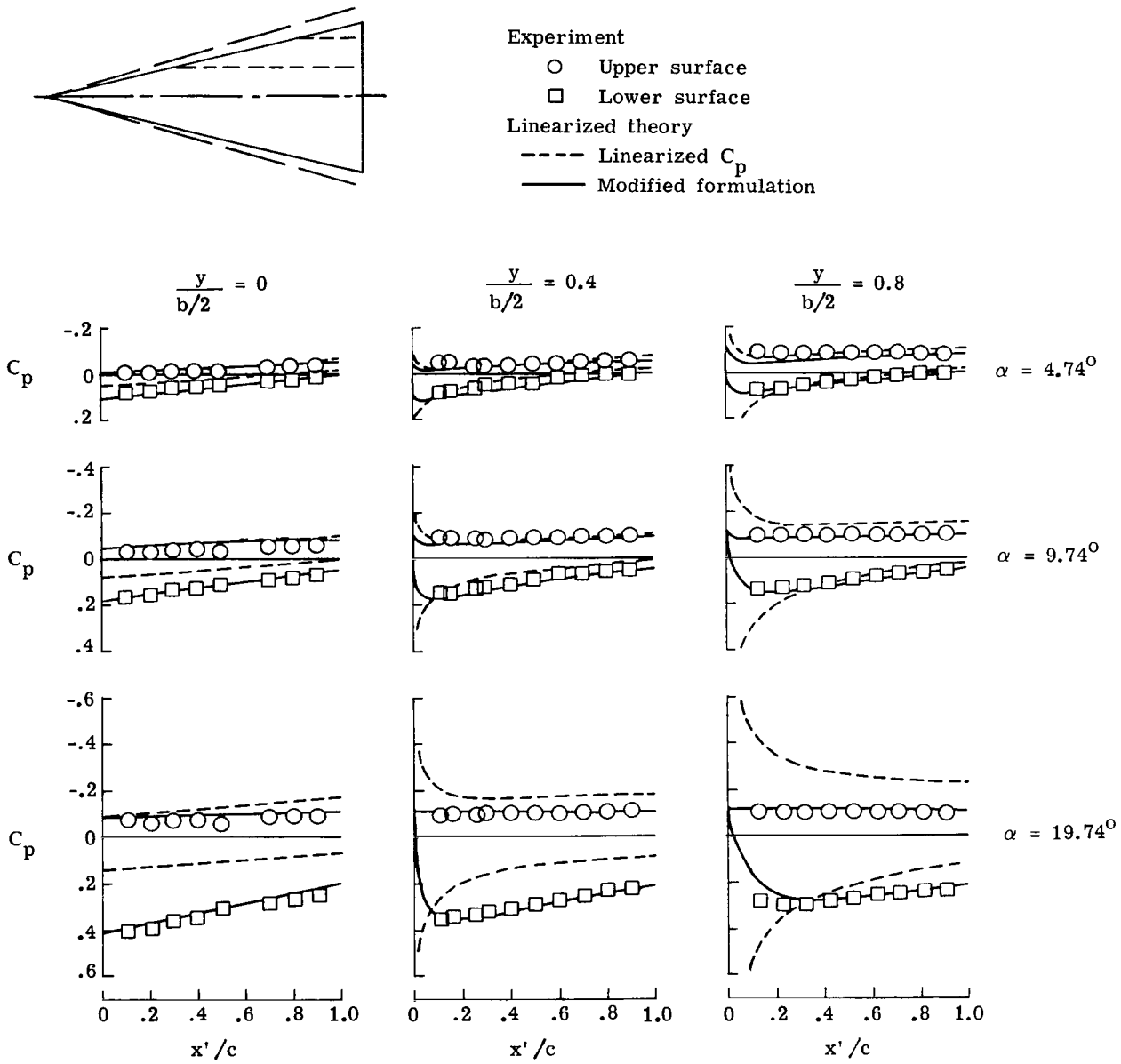

(b) $M_\infty = 3.5$.

Figure 3.- Continued.

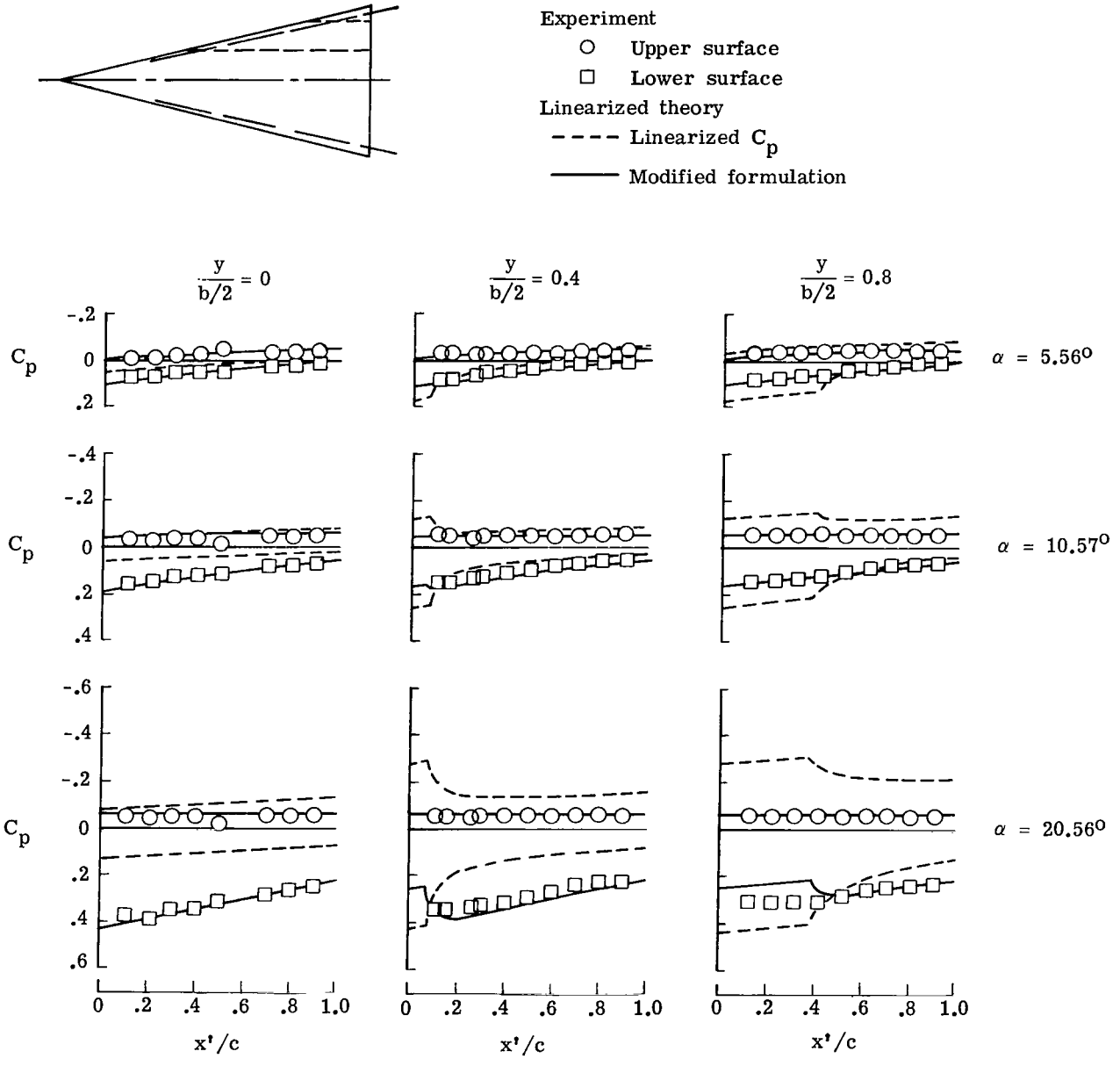

(c) $M_\infty = 4.6$.

Figure 3.- Concluded.

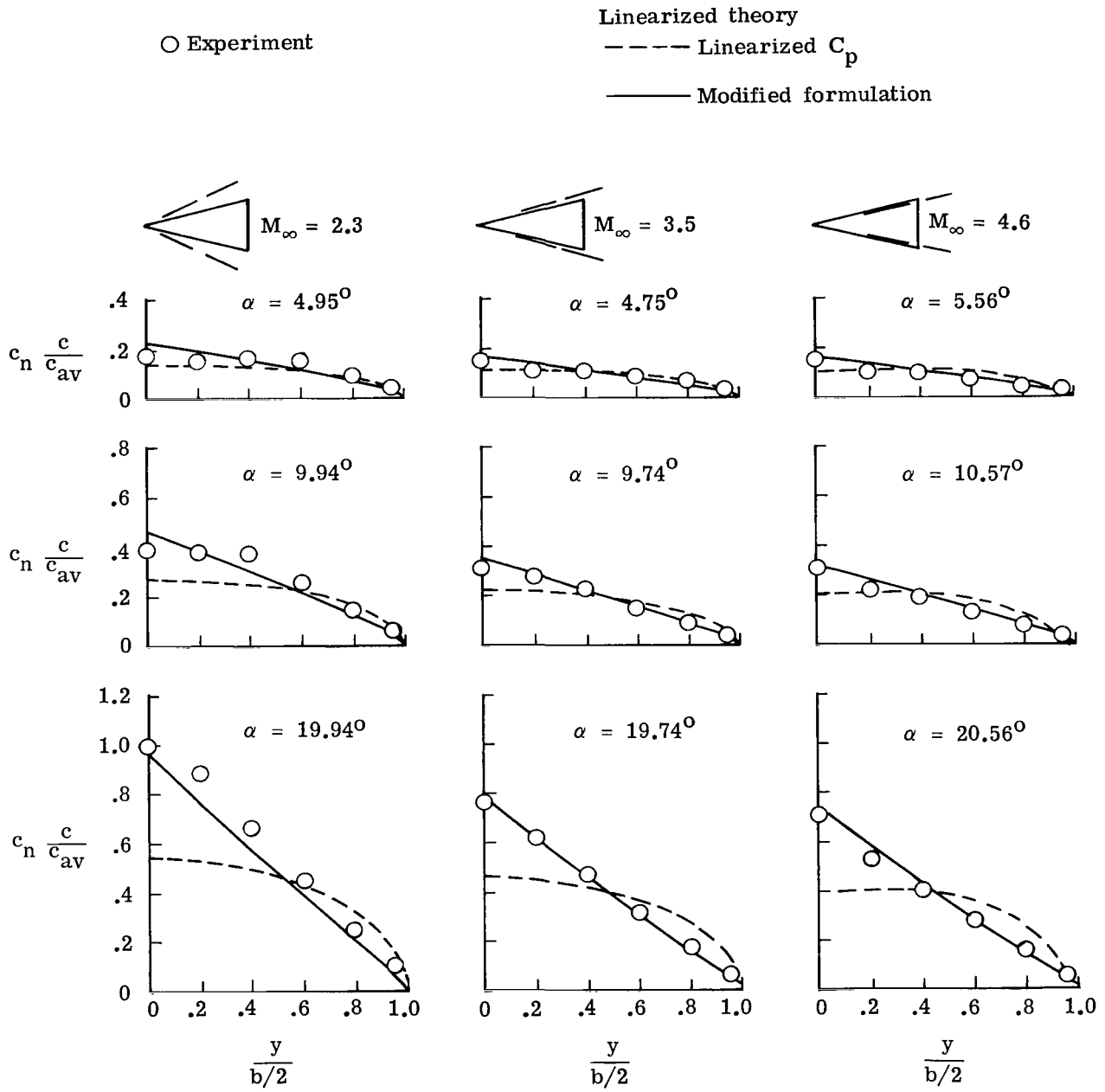

Figure 4.- Comparison of predicted and measured normal-force distributions for a delta wing with leading edge swept 76° (ref. 5).

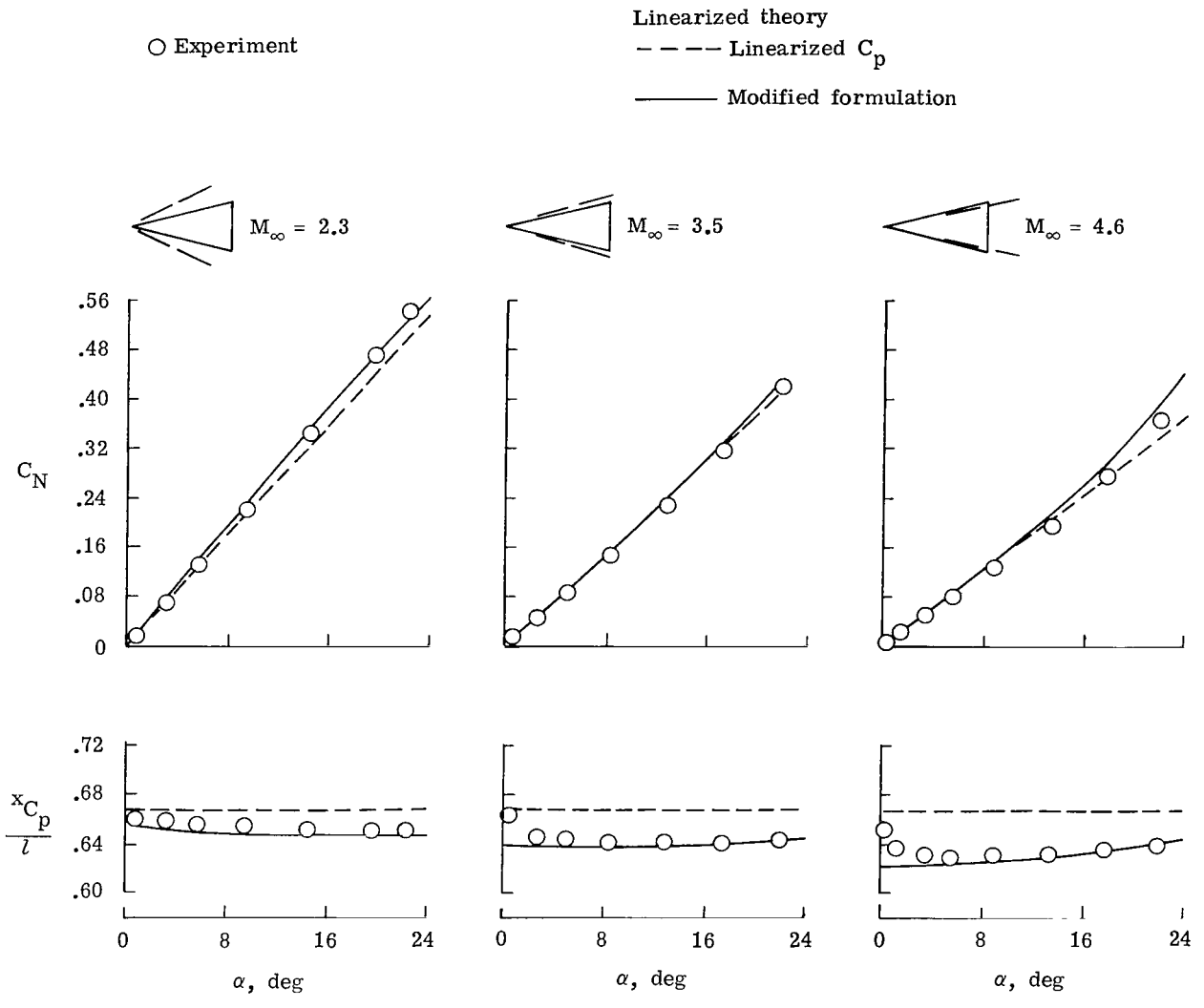

Figure 5.- Comparison of predicted and measured wing normal force and longitudinal center of pressure for a delta wing with leading edge swept 76° (ref. 5).

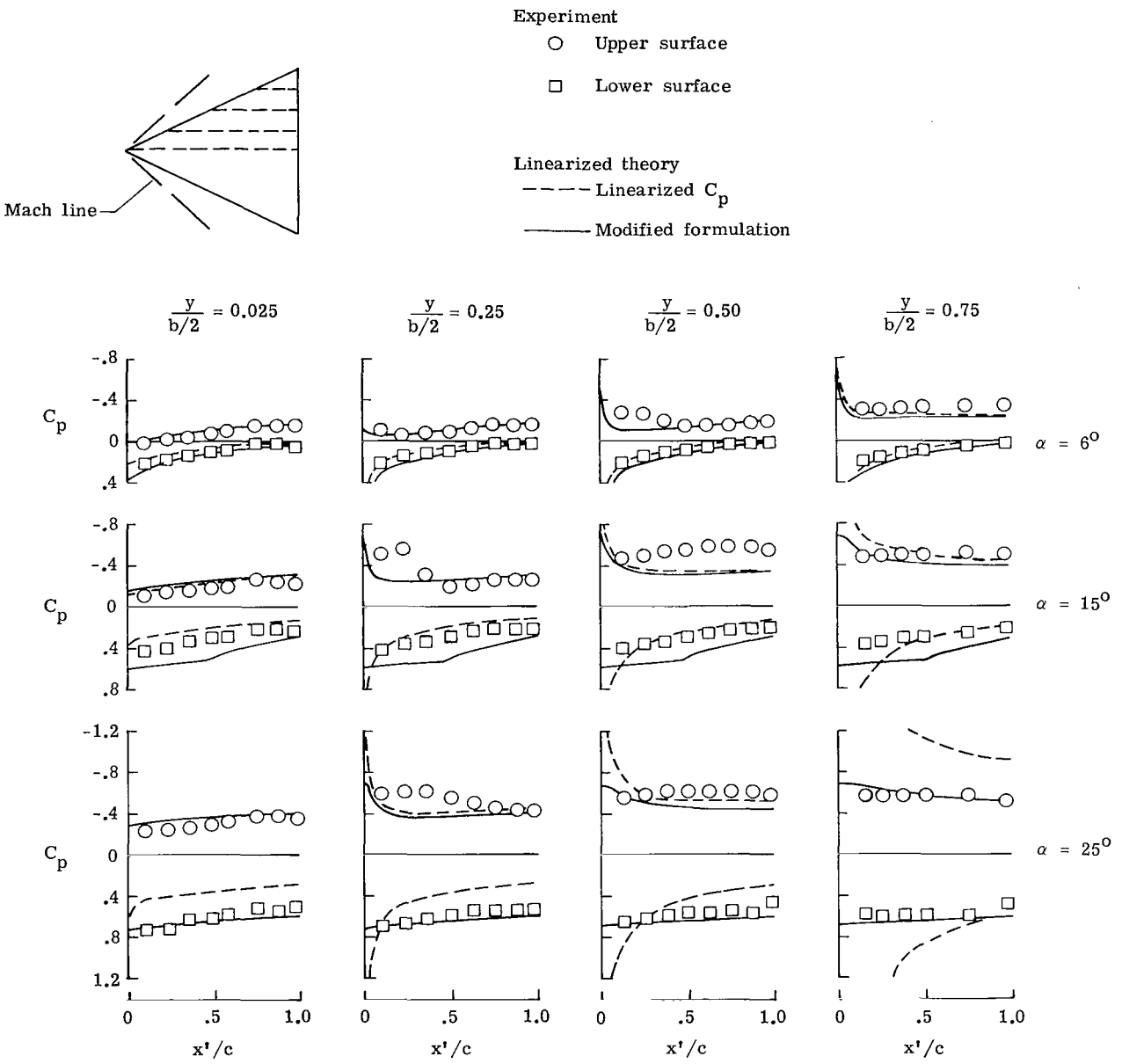

(a) M_∞ = 1.45.

Figure 6.- Comparison of predicted and measured pressure distributions for a delta wing with leading edge swept 63.4° (refs. 11 and 12).

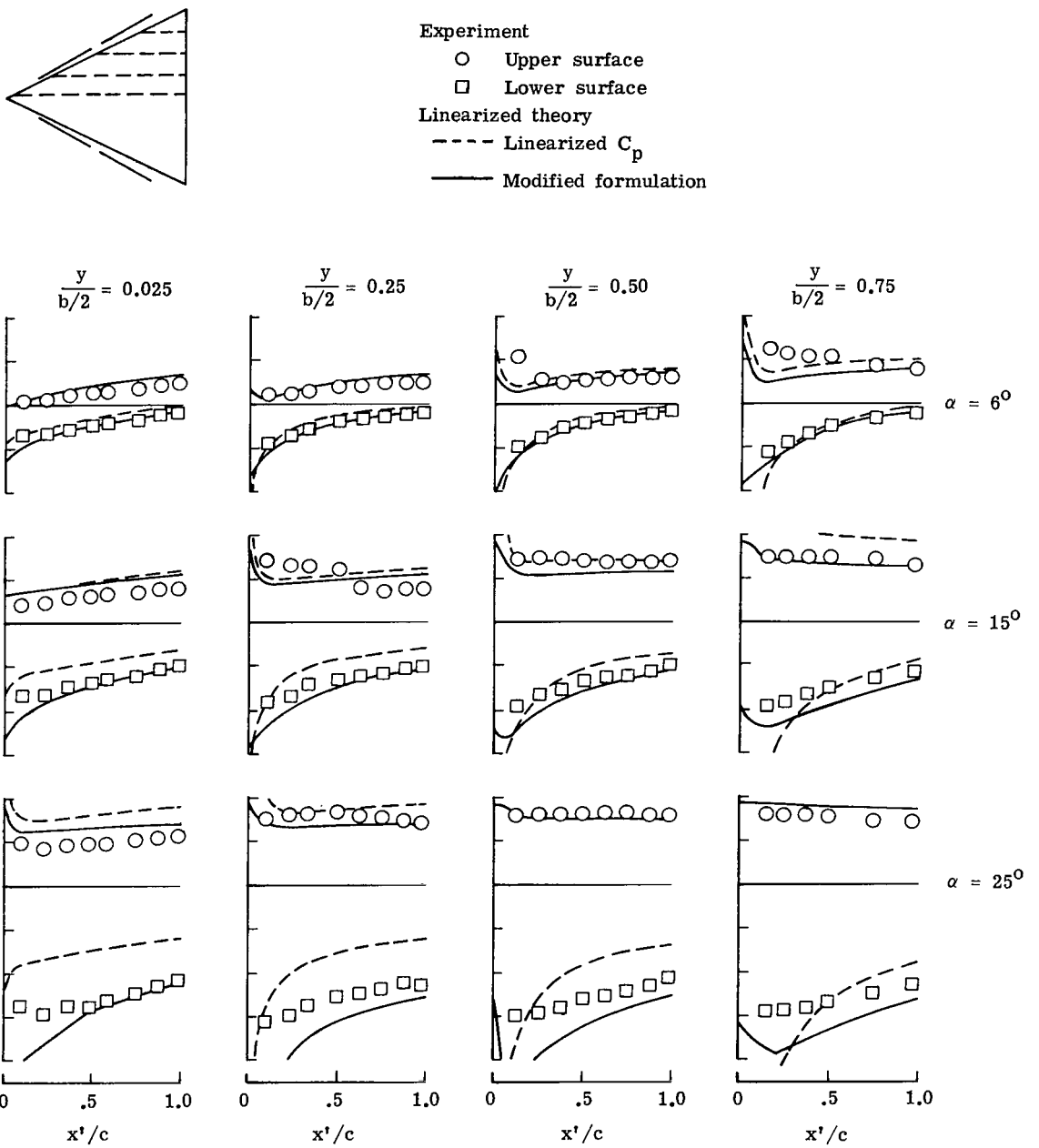

(b) $M_\infty = 1.97$.

Figure 6.- Continued.

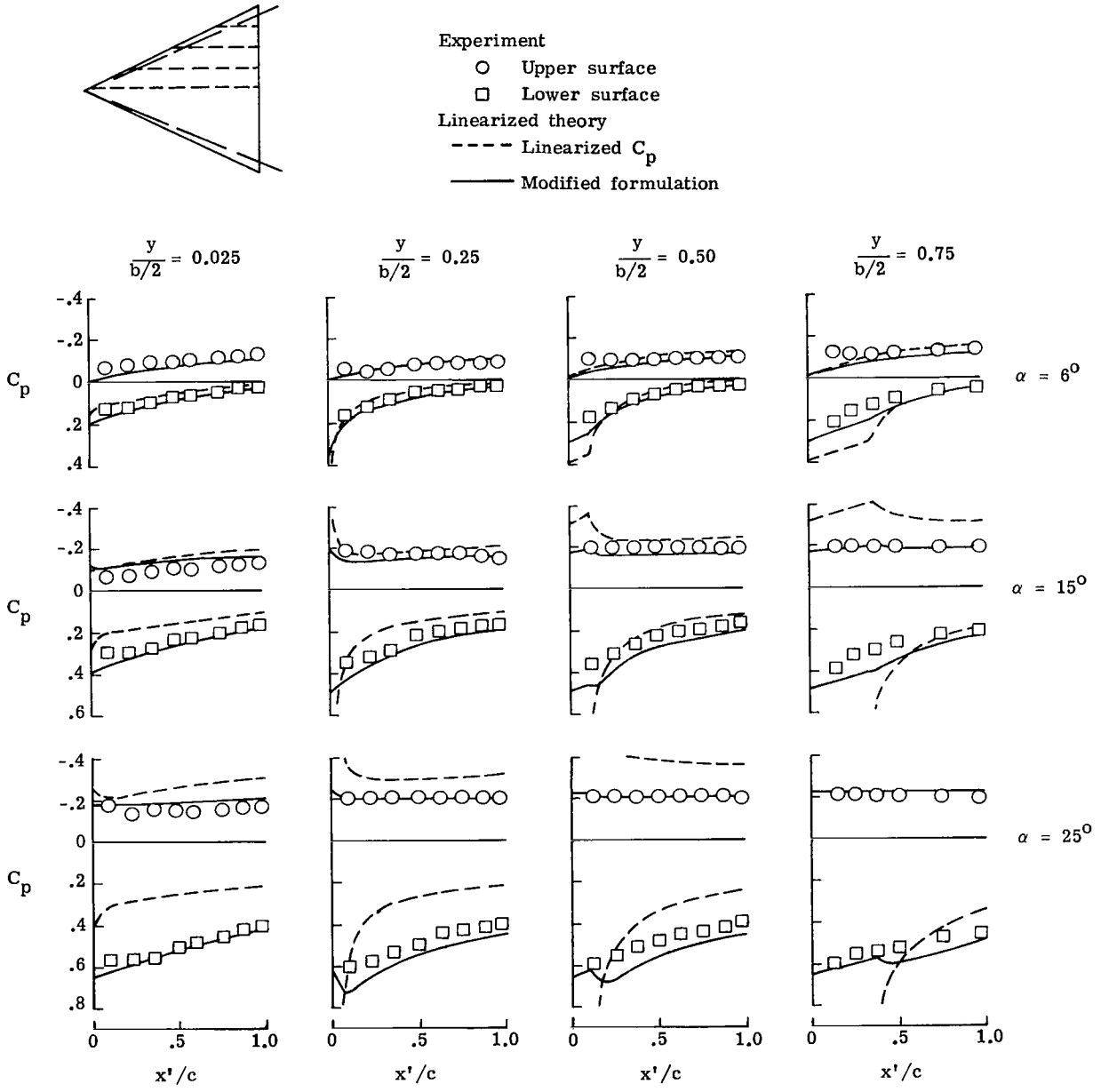

(c) $M_\infty = 2.46$.

Figure 6.- Continued.

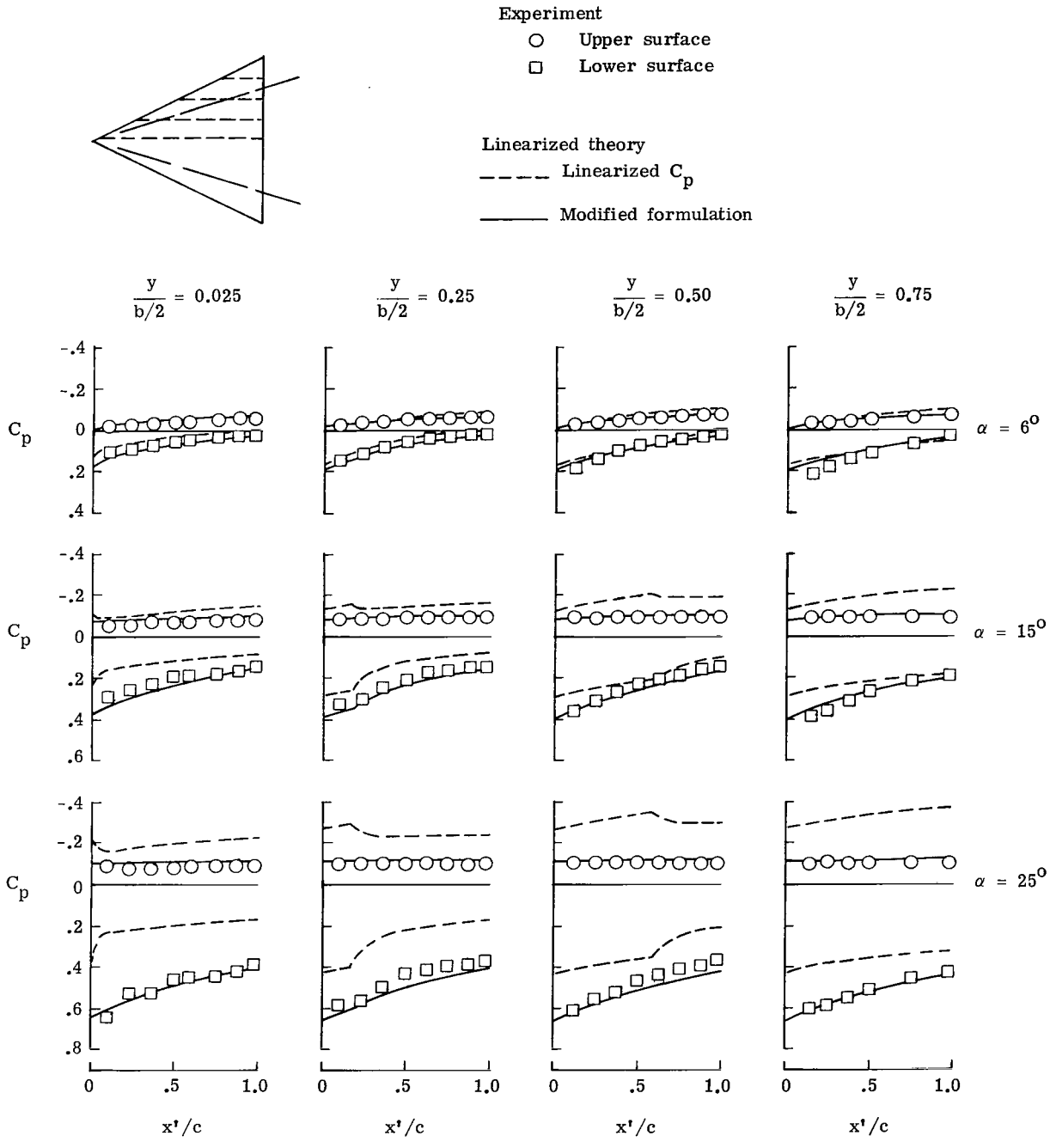

(d) M_∞ = 3.36.

Figure 6.- Concluded.

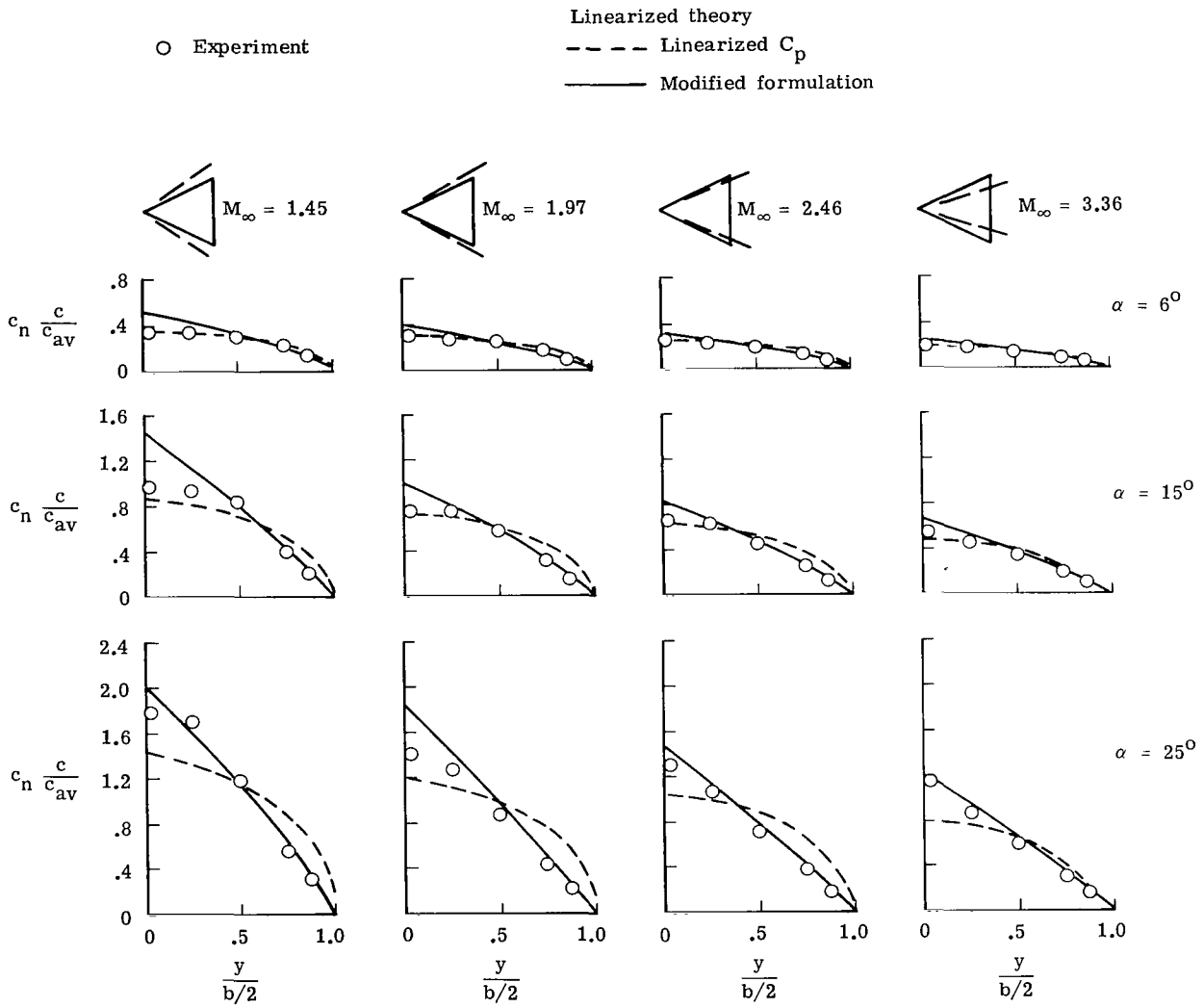

Figure 7.- Comparison of predicted and measured normal-force distribution for a delta wing with leading edge swept 63.4° (refs. 11 and 12).

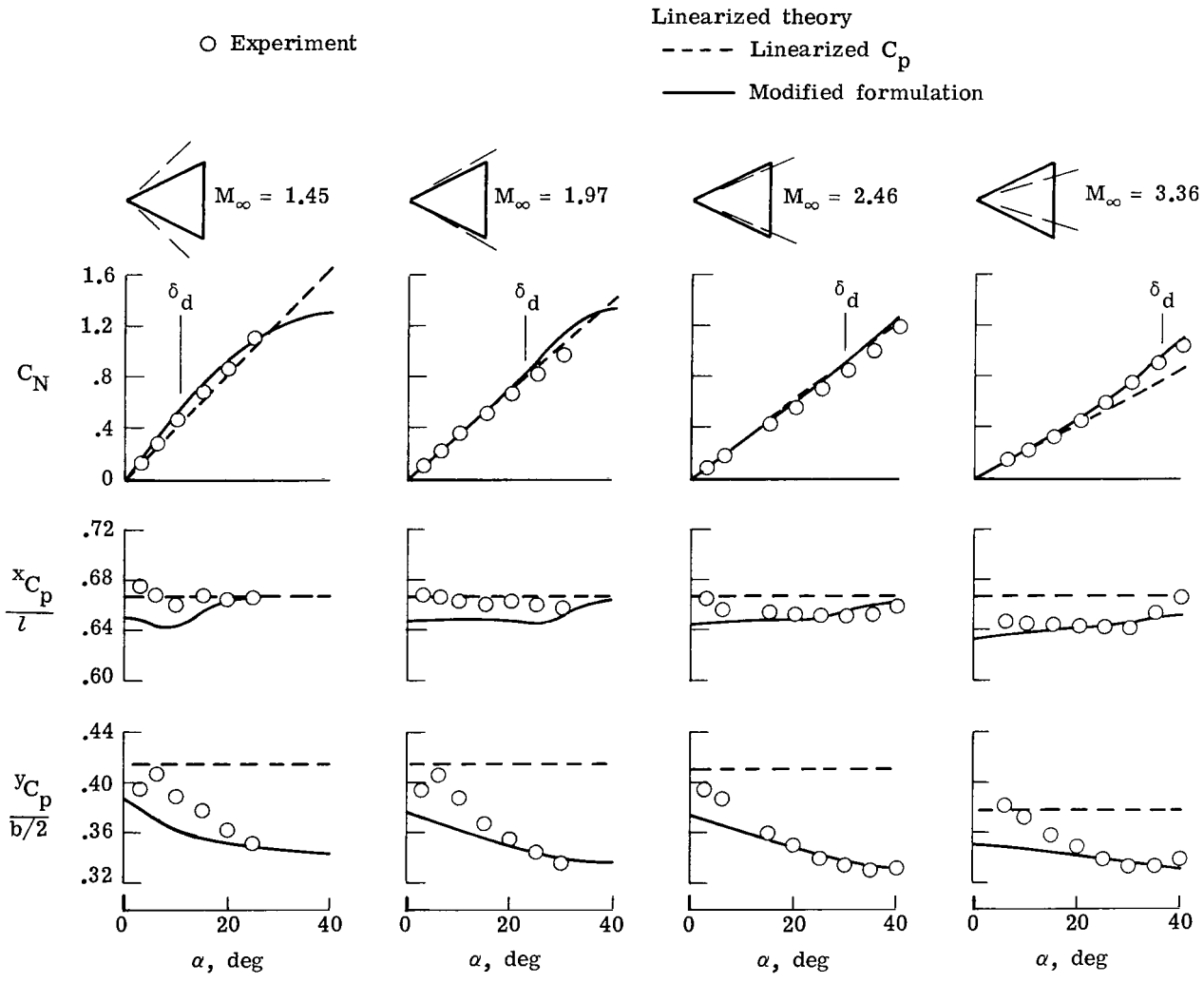

Figure 8.- Comparison of predicted and measured wing normal force and longitudinal and lateral center of pressure for a delta wing with leading edge swept 63.4° (refs. 11 and 12).

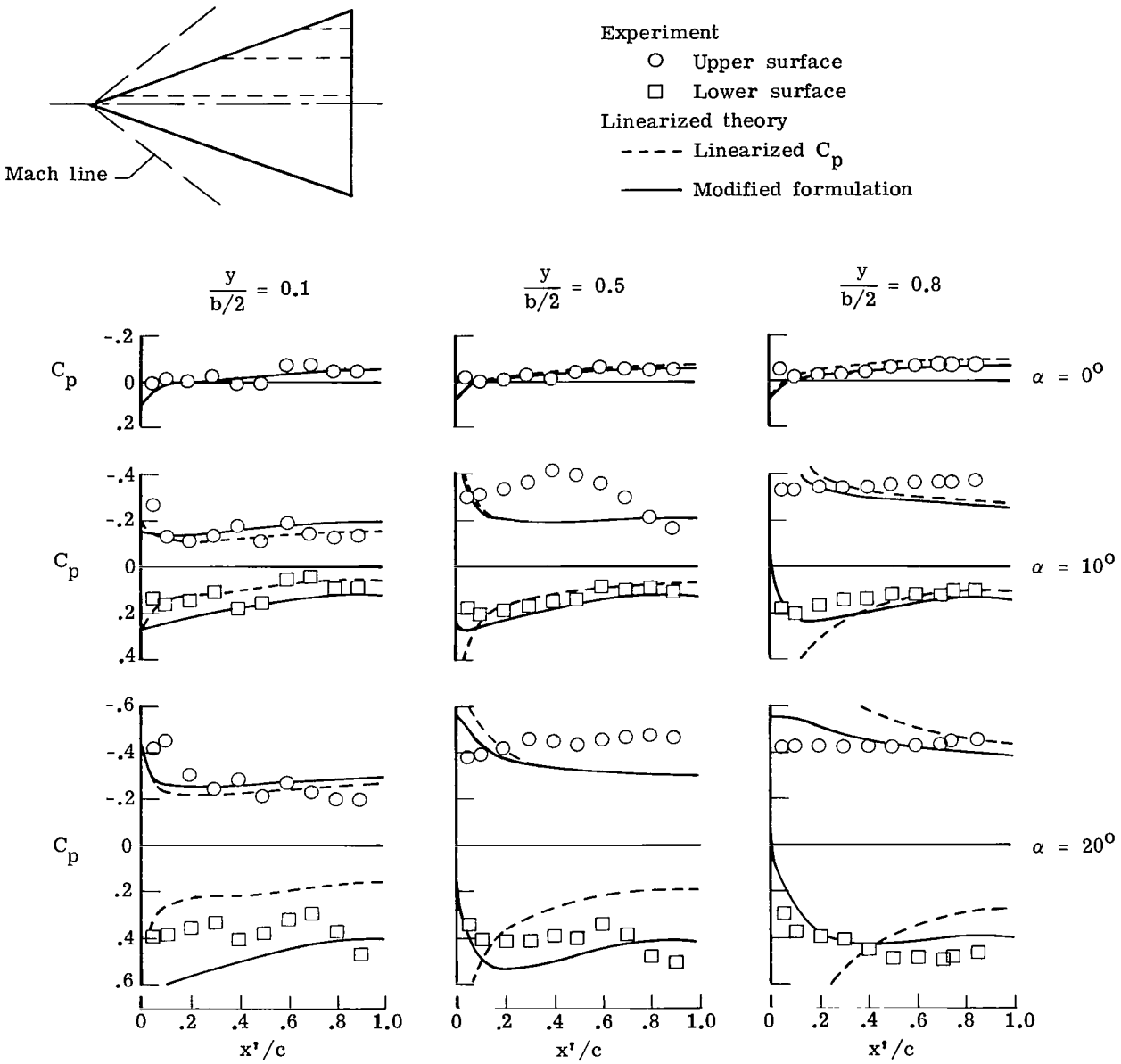

(a) M_∞ = 1.61.

Figure 9.- Comparison of predicted and measured pressure distributions for a delta wing with leading edge swept 70° (ref. 13).

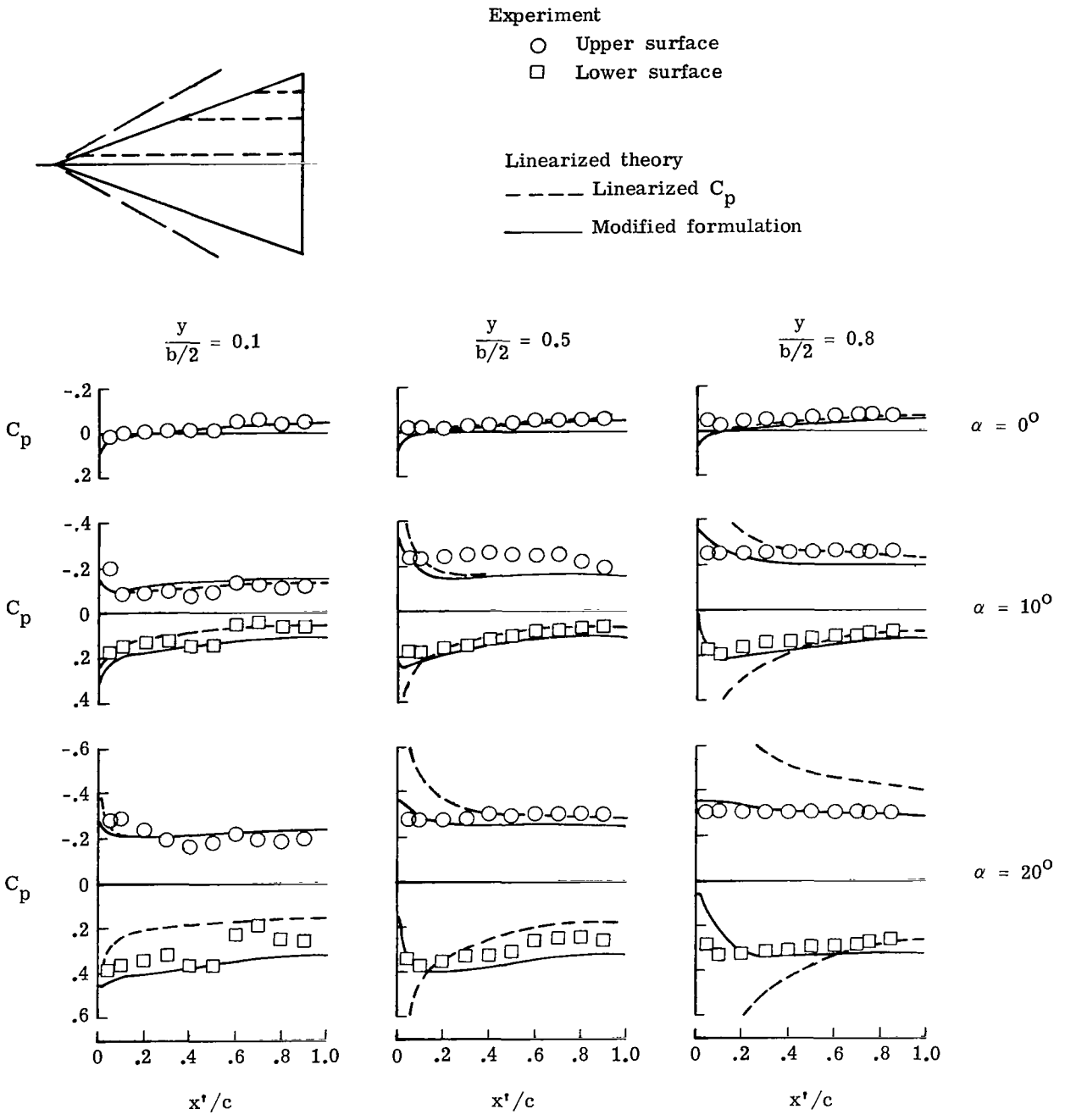

(b) M_∞ = 2.01.

Figure 9.- Concluded.

1. Report No.	2. Government Accession No.	3. Recipient's Catalog No.
NASA TP-1406		

4. Title and Subtitle
A MODIFICATION TO LINEARIZED THEORY FOR PREDICTION OF PRESSURE LOADINGS ON LIFTING SURFACES AT HIGH SUPERSONIC MACH NUMBERS AND LARGE ANGLES OF ATTACK

5. Report Date
February 1979

6. Performing Organization Code

7. Author(s)
Harry W. Carlson

8. Performing Organization Report No.
L-12654

9. Performing Organization Name and Address
NASA Langley Research Center
Hampton, VA 23665

10. Work Unit No.
505-11-13-01

11. Contract or Grant No.

12. Sponsoring Agency Name and Address
National Aeronautics and Space Administration
Washington, DC 20546

13. Type of Report and Period Covered
Technical Paper

14. Sponsoring Agency Code

15. Supplementary Notes

16. Abstract

A new linearized-theory pressure-coefficient formulation has been studied. The new formulation is intended to provide more accurate estimates of detailed pressure loadings for improved stability analysis and for analysis of critical structural design conditions. The approach is based on the use of oblique-shock and Prandtl-Meyer expansion relationships for accurate representation of the variation of pressures with surface slopes in two-dimensional flow and linearized-theory perturbation velocities for evaluation of local three-dimensional aerodynamic interference effects. The applicability and limitations of the modification to linearized theory are illustrated through comparisons with experimental pressure distributions for delta wings covering a Mach number range from 1.45 to 4.60 and angles of attack from 0° to 25°.

17. Key Words (Suggested by Author(s))
Pressure distributions
Loads prediction
Linearized theory
Delta wings
Shock expansion

18. Distribution Statement
Unclassified - Unlimited

Subject Category 02

19. Security Classif. (of this report)	20. Security Classif. (of this page)	21. No. of Pages	22. Price*
Unclassified	Unclassified	36	$4.50

* For sale by the National Technical Information Service, Springfield, Virginia 22161

NASA-Langley, 1979

National Aeronautics and
Space Administration

Washington, D.C.
20546

Official Business
Penalty for Private Use, $300

THIRD-CLASS BULK RATE

Postage and Fees Paid
National Aeronautics and
Space Administration
NASA-451

14 1 1U,A, 020279 S00903DS
DEPT OF THE AIR FORCE
AF WEAPONS LABORATORY
ATTN: TECHNICAL LIBRARY (SUL)
KIRTLAND AFB NM 87117

NASA

POSTMASTER: If Undeliverable (Section 158 Postal Manual) Do Not Return